Journal of Tissues and Materials

Modified spacer removal and optimum sintering temperature for porous magnesium scaffold fabrication

Saeid Toghyani[1], **Mohammad Khodaei**[2*]

[1]Dental Research Center, School of Dentistry, Isfahan University of Medical Sciences, Isfahan 81746-73461, Iran
[2]Department of Materials Science and Engineering, Golpayegan University of Technology, Golpayegan, Iran

Correspondence to: Khodaei M. (E-mail: khodaei@gut.ac.ir)

Abstract

Porous magnesium scaffolds have been of interest to tissue engineering researchers because of their biodegradability and biocompatibility. Space holder method is a simple method for fabrication these scaffolds, but suffer from clean spacer agent removal process. This study was conducted to introduce a modified dissolution method (Distilled water+HF acid) for the carbamide (as spacer agent) removal from inside the magnesium scaffold. Also the effect of the sintering temperature on mechanical and structural characteristics were studied by the compression test and the optical and Scanning Electron Microscopes (OM and SEM). In addition, effect on phases present in scaffold after sintering was investigated using x-ray diffraction (XRD) analysis. The results showed that the HF 48% solution is superior to that of previously used solutions (water, ethanol and sodium hydroxide) for carbamide removal, including more carbamide removal efficiency (96±2%), and partial formation of MgF_2 phase on the surface of magnesium scaffold. Also, raising the sintering temperature led to the increase of the scaffold shrinkage and the improvement of its mechanical characteristics.

Keywords: Magnesium scaffold; Tissue engineering; Powder metallurgy; Spacer agent.

Received: 30 April 2019, Accepted: 14 June 2019

DOI: 10.22034/jtm.2019.188865.1020

1. Introduction

Among body tissues, bones with porous and dense forms (cancellous and cortical) have a high potential for restoration [1]. Therefore, more than 400,000 bone grafting surgeries in Europe and around 600,000 bone grafting surgeries in U.S. are performed per year [2]. However, more than one thousand patients die in the graft waiting list [3]. On the other hand, it has been predicted that due to the increase in the road accidents and trauma injuries, implant markets growth will have been 116 billion dollars by 2020 [4]. In tissue engineering, 3D porous structures called scaffolds are used to replace the injured tissue. Actually, the scaffold acts like a temporary bed for cell adhesion and let's cells stick to it; this is followed by cells proliferation and differentiation, eventually leading to the new tissue growth and replacement [5].

Investigations on porous metals such as stainless steel, titanium and cobalt based alloys has shown that these materials have limitations including the release of metal ions and the mismatch of the Young's modulus to the surrounding bone tissue [6]. A biodegradable metal like magnesium, if used in a porous state in the body, can be degraded completely

after implantation, leading to the significant formation of a new bone and stimulating angiogenesis [2]. Moreover, this metal has some advantages such as proper biocompatibility, ability of osteoconductivit [7- 9] and cytocompatibility for new bone formation [2], low thrombogenicity, better endothelialization [10], as well as adequate elastic modulus for load bearing applications [8, 12, 13].

Of the disadvantages of this bio-metal is its rapid degradation and also the formation of a thin gray layer of magnesium hydroxide ($Mg(OH)_2$) over the surface which are in contact with a physiological solution [9]. However, when used as implant, magnesium corrosion creates a non-toxic metal oxide which is easily excreted through urine [8].

The powder metallurgy technique and the use of spacer agent particles are one of the ways in which porous magnesium scaffolds can be produced. In this method, spacer agent particles of carbamide and ammonium bicarbonate are often used as spacer agent [6, 9, 11, 13- 22]. To fabricate a high quality magnesium scaffold using carbamide ($H_2N\text{-}CO\text{-}NH_2$) spacer agent, it should all products of pyrolysis to be removed before sintering. Because pyrolysis of carbamide during sintering could release some toxic gases like ammoniac and cyanic acid (HNCO) and or solid products such as Ammelide and Ammeline, that these products decompose at temperatures much higher than magnesium sintering temperature [23]. The literatures shows that the dissolution process of spacer agent particles was performed by various solutions such as distilled water, 0.001 molar sodium hydroxide solution, and ethanol solutions [15-17]. According to previous researches [15-17], none of the previously used solutions have been able to remove the spacer particles completely, prior to the sintering process.

The current study introduced a modified dissolution method (distilled water+HF acid) for the carbamide (as spacer agent) removal; and also, the optimum sintering temperature for the fabrication of the magnesium scaffolds.

2. Materials and Methods

A magnesium powder (Merck: CAS 7439-95-4) with the purity of 99% and a particles size smaller than 50 µm was used as the scaffold matrix, and carbamide particles almost isometric (Merck: CAS 57-13-6) with the size of 700 µm were used as the space holder agent. After calculating the weight of the magnesium powder and carbamide particles for producing the magnesium scaffold with the nominal porosity of 65%, powders were carefully mixed with a small amount of ethanol (~2% in weight) as the binder and pressed in a cylinder mold with the optimum pressure of 350 MPa [15] using a 30 ton press machine. Then, in order to prevent the reaction of magnesium and carbamide particles, the carbamide particles were removed by the modified dissolution method (Distilled water twice + 48% HF solution) (Hydrofluoric acid 48%- HS Code: 28111100) before the sintering process. In order to leach the spacer agent particles out from compacted pellets, they were first soaked in distilled twice for 50 min and then for 50 min into HF solution. As soon as samples were taken out of the HF solution, the samples were cleaned with ethanol and dried for 12 hours. Afterwards, green porous samples were sintered at the temperatures of 540, 580 and 620 ℃ for 2.5 hours in a vacuum furnace (1×10^{-4} Torr) with the heating rate of 5 $\frac{℃}{min}$. After sintering, the average actual porosity was determined according to Equation (1) [24]:

$$P_a = \left(1 - \frac{\rho_f}{\rho_{Mg}}\right) \times 100 \qquad \text{Equation (1)}$$

where P_a is the actual porosity, ρ is the density of the porous sample (calculated from the dimensions and weight) and ρMg is the density of pure magnesium (1.74 g/cm^3). The weight and dimensions of the samples were measured using a digital balance of 0.0001 gram and a digital caliper with a precision of 0.01 millimeter, respectively.

In fact, $\frac{\rho_f}{\rho_{Mg}}$ is the relative density of the sintered magnesium scaffold.

XRD test with a Cu-Ka source were used to phase analyze on the surface of the magnesium sample after sintering and magnesium powder.

Scanning Electron Microscope (SEM: Philips XL-30) and optical microscope (OM: NIKON EPIPHOT

300) were used to study the microstructure and morphology of the magnesium scaffolds. The compression strength of prepared magnesium scaffolds was measured using compression testing of cylindrical samples with diameter and height of 8×8 mm. The tests were performed in accordance with ISO 13314 standard using compression strength equipment (HOUNSFIELD: H30KS) at room temperature with crosshead speed of 0.5 $mm.min^{-1}$. Each test was repeated three times and the average values were reported.

3. Results and discussion

3.1. Carbamide removal

Results of carbamide removal from inside the magnesium scaffold with 65% porosity (cold compacted at 350 MPa) were obtained by measuring the weight of the dry samples before and after the dissolution process. The results show that after 50 min immersion in distilled water twice, 70±2% of spacer agent particles (carbamide) were removed, and 22±2% of these particles were removed for 30 min immersion in HF solution. Overall, 96±2% of carbamide particles were removed during the dissolution process by the modified dissolution method for 100 min. While, according to our previous results, 50% and 70% of spacer agents were removed after 50 min immersion in NaOH solution and ethanol, respectively. In the following, only 10% and 5% of residual spacer agent particles in the pellets were removed by 0.001 molar sodium hydroxide and ethanol solutions by immersion for future 30 min, respectively. Spacer agent removal by NaOH and ethanol solutions, didn't lead to complete carbamide removal at 80 min of soaking [15]. The use of NaOH solution to remove spacer agent particles leds to oxidation of the scaffold [14, 15].

Fig. 1, presents a magnesium scaffold, sintered at 580 °C. The carbamide particles of this scaffold were removed using modified dissolution method. It is evident that the surface of scaffold is completely clean, and without any visible contamination. On the other hand, it is demonstrated that [14, 23], total thermal decomposition of urea requires temperatures above the melting point of magnesium. Also, Khodaei et. al [25], have been demonstrated that, the ammonium bicarbonate residue, cannot be removed totally from the of the pores of sintered titanium scaffold including 70 wt.% of ammonium bicarbonate at 1200 ℃. So, it is necessary to remove the spacer agent particles before the sintering process. For magnesium scaffold fabrication with lower porosity, longer dissolution time is predicted by HF solution.

Usually, initial heating cycle at 250-350 ˚C for 1-4 h were used by researchers [9, 13, 18, 26] during sintering of magnesium scaffold for carbamide removal. While, by leaching out of carbamide particles using the modified dissolution method (distilled water twice + HF solution), this step heating can be removed, and this, will lead to the reduction of time and costs of sintering process. Also this decrement, can reduce the chance of magnesium oxidation and contaminations.

Results indicated that just about 4±2% percent of carbamide was remained into closed pores (mainly in the center of sample) of magnesium scaffold after dissolution in HF that might be removed because of struts shrinkage during sintering process.

Based on the literature of review, magnesium immersion in HF for 24 h, result in formation of MgF_2 at the surface at thickness of 1.5 μm [27, 28]. Also Drynda et al. [29] reported 10-20 μm MgF_2 layer formation at the surface of Mg-Ca alloy including thick layer of $Mg(OH)_2$ after immersion in HF for 96 h, According to the equation 2 (magnesium hydroxide converted to magnesium fluoride)

Equation 2 $$Mg(OH)_2 + 2HF \rightarrow MgF_2 + 2H_2O$$

3.2. Analysis of X-ray diffraction (XRD) patterns

The X-ray diffraction patterns of initial magnesium powder and sintered magnesium scaffold at the temperature of 620℃ are shown in fig. 2(a-b). According to the Fig. 2a, X-ray pattern of initial magnesium powder, mainly consisted of pure magnesium (PDF No.: 00-035-082). In addition of small peak at 28 degree, related to magnesium oxide (periclase. PDF No.: 00-030-079). Magnesium oxide is naturally formed at the surface of magnesium powders. While at the XRD pattern of magnesium

scaffold (Fig. 2b), the peak of magnesium oxide is not observable, meaning that HF solution dissolved or

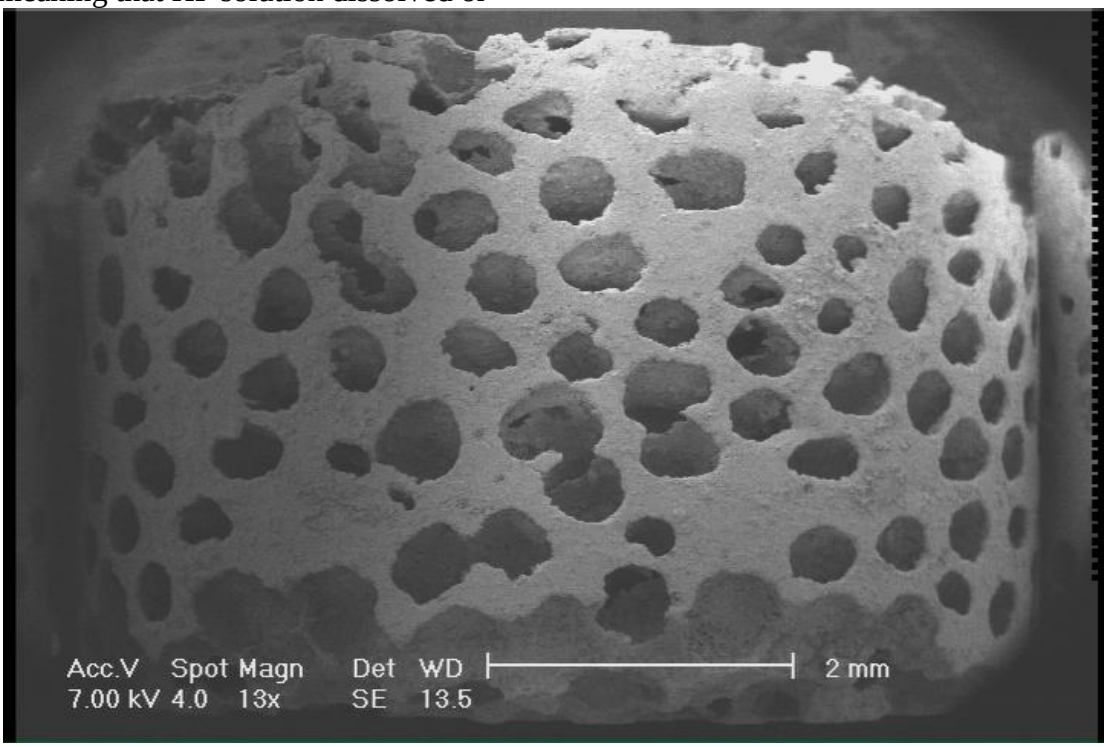

Figure 1. A sample of magnesium scaffold sintered at 580 ° C with 65% porosity (Carbamide removal by the modified dissolution method).

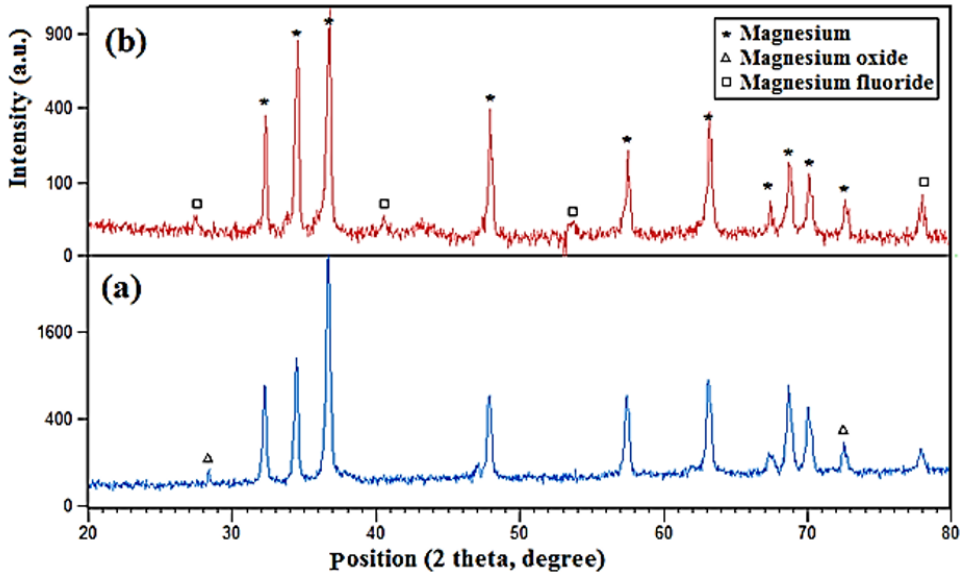

Figure 2: XRD pattern for: a) initial magnesium powder, b) sintered magnesium scaffold after carbamide removal using modified dissolution method.

removed magnesium oxide at the surface, and instead, magnesium fluoride peaks (PDF NO.: 01-070-2268) are observable. This means, a thin layer of magnesium fluoride is formed at the surface of magnesium after immersion in HF solution for 40 min. Several studies have shown that [2, 27, 41] this coating can be protected against corrosion and the release of hydrogen can be reduced due to the improved corrosion resistance of magnesium.

Based on the literature of review, small peak of magnesium oxide was observable for magnesium scaffolds, which spacer agent was removed using water base sodium hydroxide solution [15] and or thermal method [19, 21, 22, 42], at 43 degrees. So it is evident that, modified dissolution method (distilled water twice + HF solution) has more superiority than the others carbamide removal methods, because, the use of HF solution in this method leads to oxide removal or at least fewer oxidation of magnesium during spacer agent removal. According to the equation 3 and its Gibbs free energy, magnesium oxide removal by HF is reasonable.

Equation 3: $MgO\ (s) + 2HF\ (l) \rightarrow MgF_2\ (s) + H_2O\ (l)$ $\Delta G = -139$ kJ/mol [43]

It is noted that, the oxidation of MgF_2 and conversion to MgO in air occur at temperatures above 800℃ [44]. So, MgF_2 could not be decomposed during the sintering of magnesium at a protective atmosphere (vacuum or argon).

3.3. Morphology and microstructures of the magnesium scaffolds

The morphology and microstructures of the magnesium scaffolds sintered at 540, 580 and 620℃ are shown in Fig. 3.

According to SEM and OM microscope images (Fig. 3), at 530℃, the boundary between powder particles could be recognized clearly and the struts of pores are larger, while at 580℃, the boundary between the powder particles has been reduced by the migration of atoms and slightly narrowed the struts of the pores. But, it could be said that at 630℃, the boundaries between the magnesium powders has almost disappeared and the walls of pores are somewhat thinned which in some places are removed by heat.

According to the results of microscopy, increasing the temperature of sintering leads to more atomic migration at higher temperatures and more tendency to become more rigid (to reduce the free surfaces and reduce the Gibbs free energy of surface).

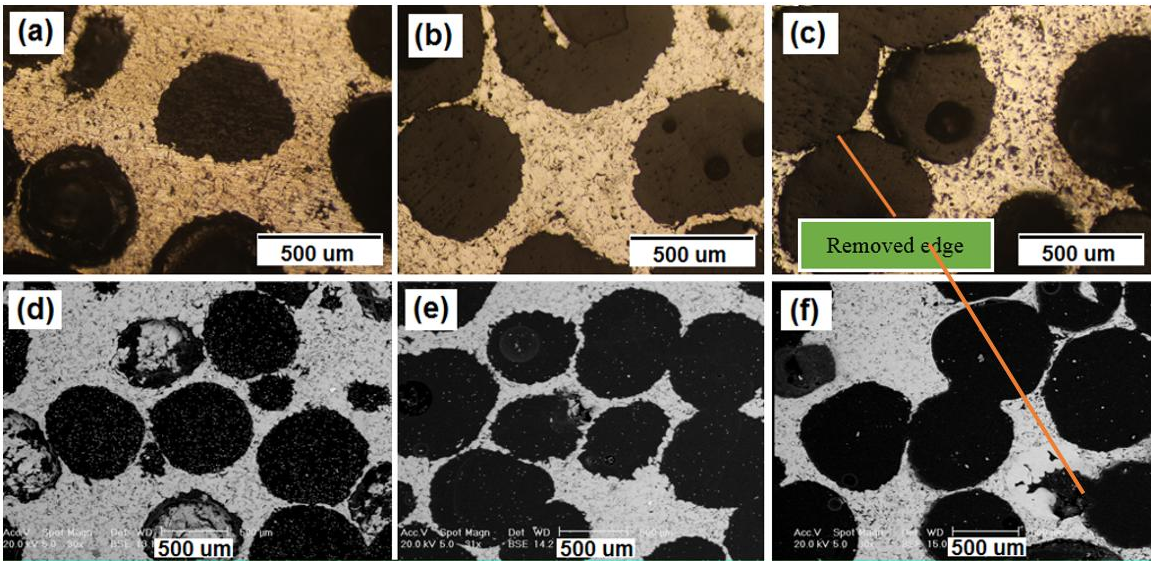

Figure 3: SEM and OM images of the magnesium scaffolds with the porosity of 65%, as sintered at 530℃ (a, d), 580℃ (b, e) and 630℃ (c, f).

3.4. Scaffolds porosity

It was observed that during the sintering process, when sintering temperature was increased to ~ 90% and ~ 96% of the pure magnesium melting point, the dimensions of the scaffolds decreased by 4% and 7%, respectively, due to shrinkage of the scaffolding during the sintering process. At sintering temperatures 90% ~ and 96% ~ melting point of magnesium, the actual porosity of the scaffolds decreased to 3% than the theoretical porosity. This can be due to the close of micropores during the sintering process or dissolution in HF solution, which results in the formation of a magnesium fluoride layer on the scaffold surfaces. So that, from microscopic pictures, it could be seen that the connection between micropores was removed due to the shrinkage of fragments.

3.5. Mechanical properties of the scaffolds

According to the curves obtained from the compression test (Fig. 4), the mechanical properties of the samples sintered at 580 and 630℃ were higher than those of the sample sintered at 530℃. Thus, as could be seen from Fig. 5 that with increasing the sintering temperature from 530 to 630℃, the mechanical properties of the sintered magnesium scaffolds were improved (approximately from 2 MPa to 6 MPa); this could be due to the development of adequate bonding between the magnesium particles. Based on the results reported by Hao et al. [17], the applicable temperature to produce magnesium scaffolds is in the range of 610-630℃. So, a much higher sintering temperature could lead to melting parts of the magnesium particles, resulting in the formation of the magnesium globules during the sintering process and the non-uniform distribution of the pore size, as well as the distortion with the undesired shape [17].

The results showed that compressive mechanical properties (average plateau stress) and the average elastic modulus were enhanced as the temperature was increased, showing the proper conformity with the mechanical properties of some cancellous bones. Table 1 shows the elastic modulus and mechanical properties of some cancellous bones [45, 46] and the results of Hao et al. [17], and Aida et al. [16], in comparison to the fabricated magnesium scaffolds in current study. Magnesium scaffolds fabricated in the current study and the researches of Hao and Aida, have been fabricated with almost same conditions and materials. According to Table 1, the results show that the magnesium scaffold that had been removed the spacer agent particles prior to the sintering process by the modified dissolution method has a higher mechanical strength than the magnesium foam produced by Hao and Aida, which removed some spacer agent particles by thermal method.

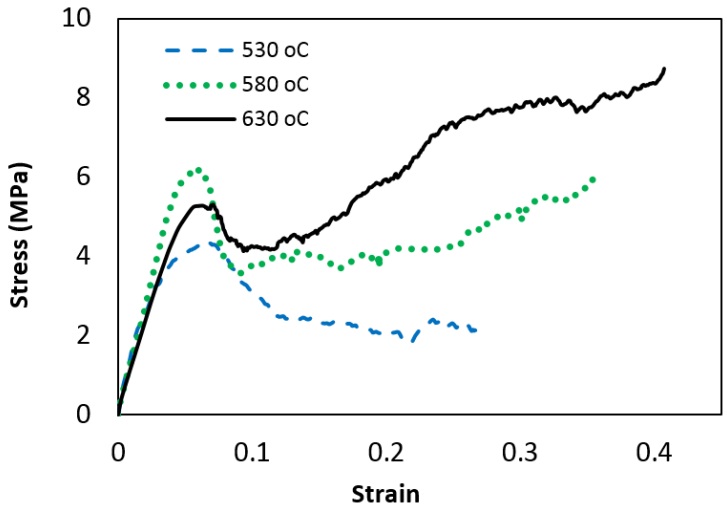

Figure 4. Engineering stress–strain curve for the compression test of the magnesium scaffolds, sintered at different temperatures.

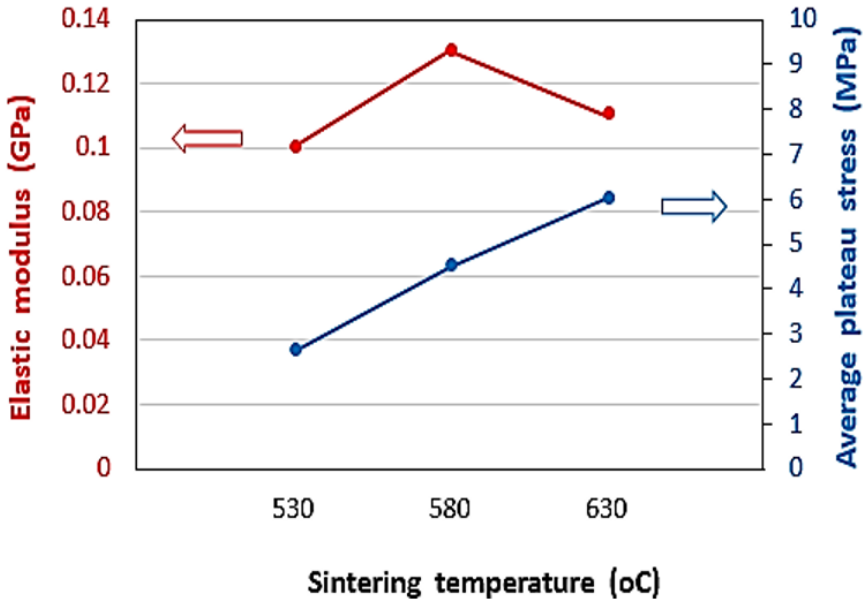

Figure5. Results of the compression test for the magnesium scaffolds.

Table 1. Mechanical properties of the magnesium scaffolds with the porosity of 65%-70%, as sintered at different temperatures, in comparison to some cancellous bones [16, 17, 45, 46].

Specimen	Sintering temperature and time (℃) & (h)	Strength (MPa)	Elastic modulus (GPa)
Cancellous bone (Femoral head)	----	1-35	--
Cancellous bone (proximal to tibia)	----	1-5	--
Cancellous bone	----	2-12	0.05-0.5
Magnesium scaffold by Hao et al.	630-2.5	4	----
Magnesium scaffold by Aida et al.	600 & 630-2.5	3.8-4.8	----
The current magnesium scaffold	580 & 630-2.5	4.48-6.00	0.11-0.13

According to the data presented in table 1, it was evident that the fabricated magnesium scaffolds in this study had mechanical properties comparable to those of the cancellous human bone; therefore, they could be a good candidate for load bearing implantation. Also, future efforts will focus on controlling the degradation rate of the magnesium porous scaffold for bone implantation.

4. Conclusion

Since determining the suitable sintering temperature and also, clean dissolution process can affect the

propertites of the magnesium porous scaffolds, the role of the sintering temperature in the microstructures of pores (micro and macro pores), and the mechanical properties of magnesium porous scaffolds was studied.
The results showed that the optimum mechanical and microstructural properties of the magnesium scaffold could be obtained by sintering at the temperature range of 580-640℃. Also, carbamide particles dissolution by modified dissolution method has more superiority in compare with the others conventional carbamide removal methods. The use of HF solution has advantages, such as removal of spacer agent particles as much as possible (about 96% ± 2%) before the sintering process, decreasing the time and costs of sintering and possible contamination of magnesium, fewer oxidation of magnesium during spacer agent removal and also improved mechanical properties.

Conflict of interest statement

The authors report no conflicts of interest.

References

[1] J. O. Hollinger, T. A. Einhorn, B. Doll & C. Sfeir, Bone Tissue Engineering, CRC Press (2004); 54-56.

[2] M-qi. Cheng, T. Wahafu, G-f. Jiang, W. Liu, Y-q. Qiao, X-c. Peng, T. Cheng, X-l. Zhang, G. He & X-y. Liu, "A novel open-porous magnesium scaffold with controllable microstructures and properties for bone regeneration", Scientific Reports-6 (2016); 1-14.

[3] R. Lanza, R. Langer & J. Vacanti, "Principles of Tissue Engineering, 2nd ed.", Academic Press, (2000).

[4] M. Prakasam, J. Locs, K. Salma-Ancane, D. Loca, A. Largeteau & L. Berzina-Cimdina, "Biodegradable Materials and Metallic Implants-A Review", Journal of functional biomaterials-8 (2017); 44-52.

[5] W. Suchanek & M. Yoshimura, "Processing and properties of hydroxyapatite-based biomaterials for use as hard tissue replacement implants", Journal of Materials Research-13 (1998); 94-117.

[6] Z.N. Husna, C.C. Lee, S. Norbahiyah & A.B. Sanuddin, "Processing and Characterization of Porous Mg Alloy for Biomedical Applications", Australian Journal of Basic and Applied Sciences-8 (2014); 160-164.

[7] H.S. Brar, M.O. Platt, M. Sarntinoranont, P.I. Martin, & M.V. Manuel, "Magnesium as a Biodegradable and Bioabsorbable Material for Medical Implants", Minerals, Metals & Materials Society-61 (2009); 31-34.

[8] M.P. Staiger, A.M. Pietak, J. Huadmai & G. Dias, "Magnesium and its alloys as orthopedic biomaterials: A review" Biomaterials-27 (2006); 1728–1734.

[9] [9] H. Zhuang, Y. Han & A. Feng, "Preparation, mechanical properties and in vitro biodegradation of porous magnesium scaffolds", Materials Science and Engineering C-28 (2008); 1462–1466.

[10] Vascular Intervention EuroPCR, PARIS, France and BUELACH, Switzerland, (2017).

[11] E. Moradi, M.E. Hosseinabadi, M. Khodaei & S. Toghyani, "Magnesium/Nano Hydroxyapatite Porous Biodegradable Composite for Biomedical Applications", Materials Research Express-6 (2019).

[12] L. Li, J. Gao & Y. Wang, "Evaluation of cyto-toxicity and corrosion behavior of alkali-heat-treated magnesium in simulated body fluid", Surface & Coatings Technology-185 (2004); 92– 98.

[13] L. Yilong, Q. Guilbao, Y. Yang, L. Xuewei & B. Chenguang, "Preparation and Compressive Properties of Magnesium Foam", Rare Metal Materials and Engineering-45 (2016); 2498-2502.

[14] J. Čapek & D. Vojtěch "Properties of porous magnesium prepared by powder metallurgy", Materials Science and Engineering C-33 (2013); 564–569.

[15] S. Toghyani & M. Khodaei, "Fabrication and characterization of magnesium scaffold using different processing parameters", Materials Research Express-5 (2018); 035407.

[16] S.F. Aida, H. Zuhailawati & A.S. Anasyida, "The Effect of Space Holder Content and Sintering Temperature of Magnesium Foam on Microstructural and Properties Prepared by Sintering Dissolution Process (SDP) using Carbamide Space Holder", Procedia Engineering-184 (2017); 290 – 297.

[17] G.L. Hao, F. S. Han & W.D. Li, "Processing and mechanical properties of magnesium foams", Journal of Porous Materials-16 (2009); 251-256.

[18] C.E. Wen, M. Mabuchi, Y. Yamada, K. Shimogima, Y. Chino & T. Asahina, "Processing of biocompatible porous Ti and Mg", Scripta Materials-45 (2001); 1147-1153.

[19] Z.S. Seyedraoufi & Sh. Mirdamadi, "Synthesis, microstructure and mechanical properties of porous Mg–Zn scaffolds", mechanical behavior of biomedical materials-21 (2013); 1-8.

[20] E. Aghion & Y. Perez, "Effects of porosity on corrosion resistance of Mg alloy foam produced by powder metallurgy technology", Materials Characterization (2014).

[21] T.H. Reddy, S. Pal, K.C. Kumarc, M.K. Mohan & V. Kokol, " Finite element analysis for mechanical response of magnesium foams with regular structure obtained by powder metallurgy method", Procedia Engineering-149 (2016); 425–430.

[22] A. Vahid, P. Hodgson & Y. Li, "New porous Mg composites for bone implants", Journal of Alloys and Compounds-724 (2017); 176-186.

[23] P.M. Schaber, J. Colson, S. Higgins, D. Thielen, B. Anspach & J. Brauer, "Thermal decomposition (pyrolysis) of urea in an open reaction vessel", Thermochimica Acta-424 (2004); 131-142.

[24] H. Bafti & A. Habibolahzadeh, "Compressive properties of aluminum foam produced by powder-carbamide spacer route", Materials and Design-52 (2013); 404-411.

[25] M. Khodaei, M. Meratian1 & O. Savabi, "Effect of spacer type and cold compaction pressure on structural and mechanical properties of porous titanium scaffold", Powder Metallurgy VOL 58, NO 2 153 (2015).

[26] C.E. Wen, Y. Yamada, K. Shimojima, Y. Chino, H. Hosokawa & M. Mabuchi, "Compressibility of porous magnesium foam: dependency on porosity and pore size", Materials Letters-58 (2004); 357–360.

[27] J. Zhang, N. Kong, J. Niu, Y. Shi, H. Li, Y. Zhou & G. Yuan, "Influence of fluoride treatment on surface properties, biodegradation and cytocompatibility of Mg–Nd–Zn–Zr alloy", J Mater Sci: Mater Med-25 (2014); 791–799.

[28] K.Y. Chiu, M.H. Wong, F.T. Cheng & H.C. Man, "Characterization and corrosion studies of fluoride conversion coating on degradable Mg implants", Surface & Coatings Technology-202 (2007); 590–598.

[29] A. Drynda, T. Hassel, Re. Hoehn, A. Perz, F.W. Bach, M. Peuster, "Development and biocompatibility of a novel corrodible fluoride-coated magnesium-calcium alloy with improved degradation kinetics and adequate mechanical properties for cardiovascular applications", Journal of Biomedical Materials Research Part A, (2009); 763-775.

[30] M.S. Uddin, C. Hall & P. Murphy, "Surface treatments for controlling corrosion rate of biodegradable Mg and Mg-based alloy implants", Sci. Technol. Adv. Mater.-16 (2015) 053501.

[31] J.H. Jo, B.G. Kang, K.S. Shin, H.E. Kim, B.D. Hahn, D.S, Park & Y.H. Koh, "Hydroxyapatite coating on magnesium with MgF2 interlayer for enhanced corrosion resistance and biocompatibility", J Mater Sci: Mater Med-22 (2011); 2437–2447.

[32] L. Mao, G. Yuan, J. Niu, Y. Zong & W. Ding, "In vitro degradation behavior and

biocompatibility of Mg–Nd–Zn–Zr alloy by hydrofluoric acid treatment", Materials Science and Engineering C-33 (2013); 242–250.

[33] W.Z. Yan, X. Ma, T. Geng, H. Wu, & Z. Li, "Mg-MOF-74/MgF2 Composite Coating for Improving the Properties of Magnesium Alloy Implants: Hydrophilicity and Corrosion Resistance", Materials-11 396 (2018).

[34] W. Yu, H. Zhao, Zhenyu Ding, Z. Zhang, B. Sun, J. Shen, S. Chen, B. Zhang, K. Yang, M. Liu, D. Chen, Y. He, "In vitro and in vivo evaluation of MgF2 coated AZ31 magnesium alloy porous scaffolds for bone regeneration", Colloids and Surfaces B: Biointerfaces-149 (2017); 330–340.

[35] H.R. Bakhsheshi-Rad, M.H. Idris, M.R. Abdul Kadir & M. Daroonparvar, "Effect of fluoride treatment on corrosion behavior of Mg-Ca binary alloy for implant application", Trans. Nonferrous Met. Soc. China-23 (2013); 699-710.

[36] P. Makkar, H.J. Kang, A.R. Padalhin, I. Park, B.G. Moon & B.T. Lee, "Development and properties of duplex MgF2/ PCL coatings on biodegradable magnesium alloy for biomedical applications", PLOS ONE | (2018).

[37] T.F. da Conceicao, N. Scharnag, C. Blawert, W. Dietzel & K.U. Kainer, "Surface modification of magnesium alloy AZ31 by hydrofluoric acid treatment and its effect on the corrosion behaviour", Thin Solid Films-518 (2010); 5209-5218.

[38] Y.C. Yang, C.Y. Tsai, Y.H. Huang, & C.S. Lin, "Formation Mechanism and Properties of Titanate Conversion Coating on AZ31 Magnesium Alloy", Journal of The Electrochemical Society-159 (5) (2012); C226-C232.

[39] Y. Yun, Z. Dong, D. Yang, M.J. Schulz, V.N. Shanov, S. Yarmolenko, Z. Xu, P. Kumta & C. Sfeir, "Biodegradable Mg corrosion and osteoblast cell culture studies", Materials Science and Engineering C-29 (2009); 1814–1821.

[40] T.F. da Conceiçao & N. Scharnagl, "Fluoride conversion coatings for magnesium and its alloys for the biological environment", Surface Modification of Magnesium and its Alloys for Biomedical Applications (2015).

[41] F. Witte, J. Fischer, J. Nellesen, C. Vogt, J. Vogt, T. Donath & F. Beckmann, "n vivo corrosion and corrosion protection of magnesium alloy LAE442", Acta Biomaterialia-6 (2010); 1792–1799.

[42] Z.S. Seyedraoufi & Sh. Mirdamadi, "In vitro biodegradability and biocompatibility of porous Mg-Zn scaffolds coated with nano hydroxyapatite via pulse electrodeposition", Trans. Nonferrous Met. Soc.China-25 (2015); 4018-4027.

[43] Grise, "Corrosion of Ceramics in Aqueous Hydrofluoric Acid", Journal of the American Ceramic Society-83 (2000); 1160-1164.

[44] H.K. Chen, Y.Y. Jie & L. Chang, "Oxidation characteristics of MgF2 in air at high temperature", IOP Conference Series: Materials Science and Engineering-170 (2017); 012035.

[45] D.M. Liu, "Porous Hydroxyapatite Bioceramics", Key Engineering Materials-115 (1996); 209-232.

[46] S.C.P. Cachinho & R.N. Correia, "Titanium scaffolds for osteointegration: mechanical, in vitro and corrosion behaviour, J Mater Sci: Mater Med-19 (2008); 451-457.